© The American Society of Gene Therapy

Injection of Bone Marrow Cell Extract Into Infarcted Hearts Results in Functional Improvement Comparable to Intact Cell Therapy

Yerem Yeghiazarians[1], Yan Zhang[1], Megha Prasad[1], Henry Shih[1], Shereen A Saini[1], Junya Takagawa[1], Richard E Sievers[1], Maelene L Wong[1], Neel K Kapasi[1], Rachel Mirsky[1], Juha Koskenvuo[1], Petros Minasi[1], Jianqin Ye[1], Mohan N Viswanathan[1], Franca S Angeli[1], Andrew J Boyle[1], Matthew L Springer[1] and William Grossman[1]

[1]*Division of Cardiology, Department of Medicine, University of California–San Francisco, San Francisco, California, USA*

We compared therapeutic benefits of intramyocardial injection of unfractionated bone marrow cells (BMCs) versus BMC extract as treatments for myocardial infarction (MI), using closed-chest ultrasound-guided injection at a clinically relevant time post-MI. MI was induced in mice and the animals treated at day 3 with either: (i) BMCs from green fluorescent protein (GFP)-expressing mice (n = 14), (ii) BMC extract (n = 14), or (iii) saline control (n = 14). Six animals per group were used for histology at day 6 and the rest followed to day 28 for functional analysis. Ejection fraction was similarly improved in the BMC and extract groups versus control (40.6 ± 3.4 and 39.1 ± 2.9% versus 33.2 ± 5.0%, $P < 0.05$) with smaller scar sizes. At day 6 but not day 28, both therapies led to significantly higher capillary area and number of arterioles versus control. At day 6, BMCs increased the number of cycling cardiomyocytes (CMs) versus control whereas extract therapy resulted in significant reduction in the number of apoptotic CMs at the border zone (BZ) versus control. Intracellular components within BMCs can enhance vascularity, reduce infarct size, improve cardiac function, and influence CM apoptosis and cycling early after therapy following MI. Intact cells are not necessary and death of implanted cells may be a major component of the benefit.

Received 25 November 2008; accepted 25 March 2009; published online 21 April 2009. doi:10.1038/mt.2009.85

INTRODUCTION

Myocardial infarction (MI), ischemic cardiomyopathy, and congestive heart failure remain prominent health challenges worldwide. Despite therapeutic advances, there are currently no approaches in clinical practice that replace myocardial scar with functioning contractile tissue.[1–3] Cell therapy using cells derived from BM following MI has shown promise in reducing the size of the infarct and improving cardiac function. However, the mechanism of action of such cell therapies remain highly controversial.[4–10] Many have postulated that the mechanism of action of BM cell (BMC) therapy is via release of paracrine factors. Importantly, implanted cells have not been shown to survive in myocardium for long periods. Whether they can survive long enough to synthesize the paracrine factors necessary to effect cardiac repair, or whether they release preformed cellular contents, perhaps even in the act of dying, is not known.

One of the main limitations of the preclinical small animal studies is the inability to deliver the cells to the infarcted hearts at clinically relevant times after MI because of the excessive mortality associated with a second open-chest surgical approach. However, results from the recently reported Reinfusion of Enriched Progenitor Cells and Infarct Remodeling in Acute Myocardial Infarction Trial[11] suggest the optimal time for cell therapy is ≥5 days after MI with little benefit derived from early treatment. In most small animal experiments, the cells have been delivered at the time of infarction or within several hours, usually when the chest is already open for the induction of the infarct. Moreover, injection of cells into the ~1-mm thick myocardial wall presents a challenge because of the potential for inaccurate injections and intracavitary loss of cells.[12,13] No method to date has been available to confirm that the injection is entirely intramyocardial rather than intraventricular. Dawn and Bolli[12] have stated that "this (injection), even in the best hands, is only partly successful" and Kajstura *et al.*[13] observed that the success rate of intramyocardial injection is ~50%. We recently developed an ultrasound-guided injection technique for use in the mouse MI model.[14] Using this novel approach, we can accurately visualize the peri-infarct borders and deliver cells into the myocardium in a closed-chest fashion with a high success rate. We can also remove the animals with unsuccessful injections (*i.e.*, left ventricular cavity injection) from the study at the time of the injection to assure uniformity of optimal injections in the studied groups. Importantly, this approach has allowed us to perform studies at a more clinically relevant time-point by injecting the hearts several days post-MI without significant mortality. Based on the qualitative and quantitative information about the natural history of post-MI cardiac inflammation and remodeling in mice,[15] we delivered the therapies 3 days

Correspondence: *Yerem Yeghiazarians, Division of Cardiology; Box 0103, University of California–San Francisco, San Francisco, California 94143-0103, USA. E-mail: yeghiaza@medicine.ucsf.edu*

© The American Society of Gene Therapy

after MI. As this is similar to days 6–7 post-MI in the human,[15] the resulting unique experimental model mimics the crucial conditions of the human trials. In addition, we wanted to evaluate the whole BM and the extract derived from the whole BM rather than using the mononuclear component. We hypothesized that if a paracrine mechanism is at play, use of the whole BM and the whole BM-derived extract would enable us to detect the effects of any likely protein or any factor that would potentially be released by any cell type.

In this study, we lysed BMCs and removed the insoluble material, leaving only the intracellular contents. Next, using ultrasound-guided injections, we compared injection of living whole BMCs versus whole BMC extract on infarct size and cardiac function at day 28 post-MI. After observing a similar improvement in both groups, we sought to discover the mechanism of this improvement in each group and conducted a detailed analysis of blood vessel density, cardiomyocyte (CM) apoptosis, and proliferation within the first week after therapy.

RESULTS

BMCs and BMC extract reduced infarct size and resulted in improvement in cardiac function

Both BMC and extract groups had significantly smaller histologic infarct size at day 28 versus the control group (24.4 ± 7.3 and 24.3 ± 12.8% versus 37.9 ± 11.1%, $P = 0.02$ and $P = 0.05$, respectively; **Figure 1**). Left ventricular ejection fraction (LVEF) was uniformly reduced from an average of 57.2 ± 4.2% before MI to 38.4 ± 3.5% ($P < 0.001$) at 2 days post-MI in all groups, with no significant differences amongst the groups (**Figure 2**). At 28 days post-MI, LVEF improved significantly in both the BMC and extract groups versus Hank's buffered saline solution (HBSS) (40.6 ± 3.4 and 39.1 ± 2.9% versus 33.2 ± 5.0%, $P < 0.05$). There was no significant difference between the BMC versus extract groups. There was less ventricular dilatation in the cell injection group compared with controls (end-systolic volume: 51.2 ± 8.5 µl versus 70.5 ± 14.0 µl, $P = 0.005$; end-diastolic volume: 85.2 ± 10.0 µl versus 105.0 ± 15.8 µl, $P = 0.01$) (**Figure 2**). Furthermore, there was significantly less peri-infarct wall thinning in the BMCs injection group compared with controls (0.53 ± 0.06 mm versus 0.39 ± 0.08 mm, $P = 0.005$). There were no statistically significant differences in the posterior wall thickness (0.76 ± 0.09 mm versus 0.72 ± 0.07 mm, P = NS) or infarct scar thickness (0.24 ± 0.05 mm versus 0.21 ± 0.05 mm, P = NS) between the BMC and control groups, respectively.

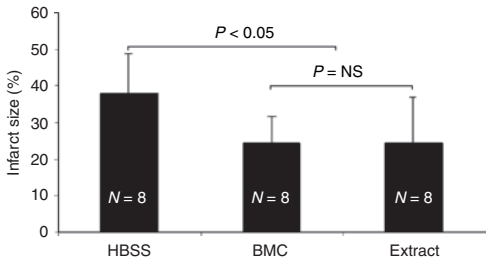

Figure 1 Limitation of infarct size in BMC and extract groups. Infarct size was determined morphometrically in trichrome-stained sections. Bars show mean ± SD. BMC, bone marrow cells; HBSS, Hank's buffered saline solution; NS, not significant.

The improvement of LVEF in the extract group was also associated with less ventricular dilatation as demonstrated by smaller end-systolic volumes versus controls (55.8 ± 11.2 µl versus 70.5 ± 14.0 µl, $P = 0.04$) (**Figure 2**). The changes in the EDVs favored the extract group but did not reach statistical significance compared with controls (91.2 ± 14.2 µl versus 105.0 ± 15.8 µl, $P = 0.09$). In addition, there was significantly less peri-infarct wall thinning in the extract group compared with the control (0.50 ± 0.06 versus 0.39 ± 0.08 mm, $P = 0.01$), but no statistically significant difference in the posterior wall thickness between the groups

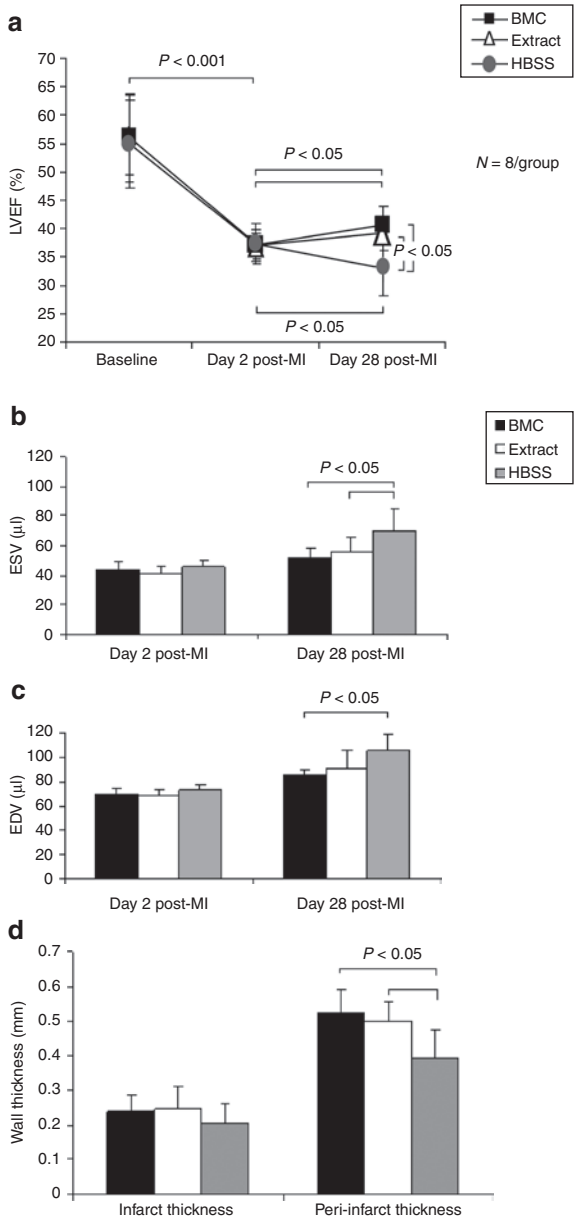

Figure 2 Therapeutic effect of BMCs and extract on left ventricular function measured by echocardiography. (**a**) LVEF; each line represents the mean of one experimental group. (**b**) ESV, and (**c**) EDV at day 28. (**d**) Wall thickness of the peri-infarct region and the infarct scar. Data are shown as mean ± SD; $N = 8$/group. BMC, bone marrow cells; EDV, end-diastolic volume; ESV, end-systolic volume; HBSS, Hank's buffered saline solution; LVEF, left ventricular ejection fraction; MI, myocardial infarction.

© The American Society of Gene Therapy

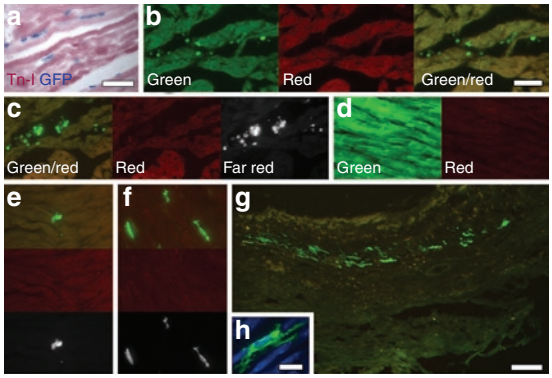

Figure 3 Conclusive detection of GFP-expressing cells by colorimetric and multicolor fluorescence approaches. (**a**) GFP$^+$ cells were detected 3 days after implantation (blue stain). There was no colocalization of GFP with troponin-I (Tn-I; red stain) in any cells. (**b**) Positive control for GFP fluorescence from implantation of GFP$^+$ BMCs with immediate harvest. Intrinsic GFP fluorescence is shown with the green filter, red filter, and a green/red merged image. Autofluorescence is both green and red, while GFP$^+$ cells are only green; the merged image shows green cells against a yellow background. (**c**) Adjacent section immunostained for GFP using a far-red secondary antibody and a green tertiary antibody, presented as green/red merged image, red filter, and far-red filter. GFP$^+$ cells are identified as those that are green, are not red, and are far red, with the absence of signal in the red image controlling for wide-spectrum artifactual background fluorescence. (**d**) Positive control staining for GFP in hearts from GFP transgenic mice, with signal in green and no signal in red. (**e**) Rare GFP$^+$ cell in border-zone myocardium 25 days after injection, in green/red, red, and far-red colors. (**f**) A similar presentation of rare GFP$^+$ cells in the infarct scar. (**g**) Low magnification image of the largest cluster of GFP$^+$ cells that we could detect in the infarct scar, green/red merged image. Clusters of this size were not observed in most hearts injected. (**h**) High magnification image of a representative GFP$^+$ cell in the infarct scar, with nuclei in blue. Bar = 50 µm for (**a–f**) at equal magnification; Bar = 100 µm (**g**) and 10 µm (**h**). GFP, green fluorescent protein.

(0.68 ± 0.05 mm in the extract group versus 0.72 ± 0.07 mm in the control group, $P = 0.09$).

Implanted BMCs did not differentiate into CMs and GFP$^+$ cells were rarely present at day 28

Because the BMCs were isolated from a green fluorescent protein (GFP) transgenic C57BL/6 strain, we attempted to detect GFP$^+$ cells in the implanted regions and to determine the identity of any such cells observed. Sections were stained with antibodies to GFP and counterstained with anti-troponin-I antibodies on day 6 post-MI (**Figure 3a**). GFP$^+$ cells were detected within the infarct zone and border zone (BZ) in all animals in the BMC group and in none of the extract group, indicating that GFP$^+$ cells were able to persist for at least 3 days after injection. No GFP$^+$ CMs were observed.

To gain insight as to how the functional benefits of BMCs were achieved, we sought to determine the fate of the implanted cells at day 28. To avoid artifacts caused by tissue autofluorescence,[16] we used both intrinsic GFP fluorescence and a two-color immunofluorescence approach (see Materials and Methods), in which GFP was detected in both green and far-red fluorescent wavelengths and confirmed by the absence of signal in the red fluorescent wavelength as a negative control, to distinguish from autofluorescence (**Supplementary Figure S1** shows representative artifact). Positive controls consisting of hearts harvested immediately after

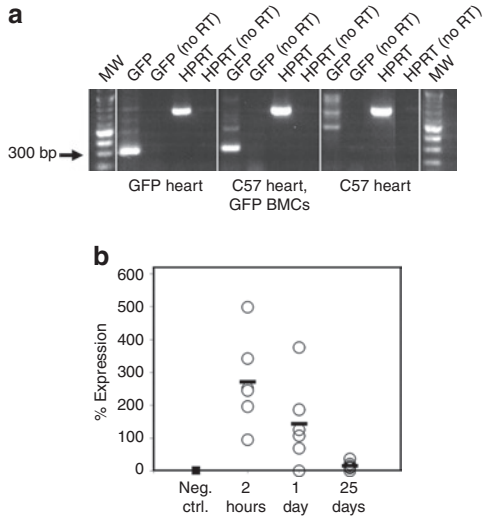

Figure 4 Disappearance of GFP transcripts over time. (**a**) RT-PCR controls showing GFP PCR product (307 base pairs) and HPRT reference gene with and without reverse transcription (RT), from GFP transgenic heart, wild type heart plus GFP$^+$ BMCs, and wild type heart negative control. (**b**) Quantitative RT-PCR (TaqMan) of GFP with histone 3.3A reference gene in six hearts per group harvested at 2 hours, 1 day, and 25 days after injection, shown with a negative control lacking GFP$^+$ cells ($P = 0.001$, 2 hours versus 25 days). GFP transcripts are almost undetectable by day 25. *Y*-axis shows GFP percent relative expression to the histone reference gene. BMC, bone marrow cells; GFP, green fluorescent protein; HPRT, hypoxanthine phosphoribosyltransferase; neg. ctrol., negative control.

implantation of GFP$^+$ BMCs exhibited clusters of cells that fit these criteria, further confirmed with colorimetric immunohistochemical staining for GFP (**Figure 3b,c**). As an additional positive control, GFP$^+$ CMs were easily detected in heart tissue sections from the GFP-expressing transgenic mice from which the BMCs were derived, as expected (**Figure 3d**; **Supplementary Figure S2** is an expanded figure of this). However, in the hearts implanted with GFP-expressing BMCs, GFP$^+$ CMs were not observed, despite perfusion fixation that preceded harvest to ensure retention of the GFP.[16] We did observe very few individual GFP$^+$ cells in the myocardium near the implantation site and in the infarct scar, with rare clusters of these cells in the scar (**Figure 3e–h**; panel **g** shows the largest cluster detected but this was the exception). These cells did not stain positive for the macrophage marker F4/80 nor the pan-hematopoietic marker CD45, as well as common identification markers of CMs, endothelial cells, smooth muscle cells, myofibroblasts, and pericytes (see Materials and Methods). Thus, their identity could not be established. Such cells were not detected in the negative control group that had not been injected with GFP-expressing cells, further confirming that the rare positive cells observed in the BMC-implanted hearts were expressing GFP. Additionally, persistence of GFP transcripts was monitored by quantitative reverse transcription–PCR (RT-PCR) in individual hearts harvested at varying times after implantation (**Figure 4**). The average level of GFP RT-PCR products decreased over the first day and was almost entirely gone by day 25 postimplantation, confirming that BMCs were present initially and mostly disappeared over the course of the experiment. These data indicate that the BMCs caused functional improvement despite only minimal long-term retention.

© The American Society of Gene Therapy

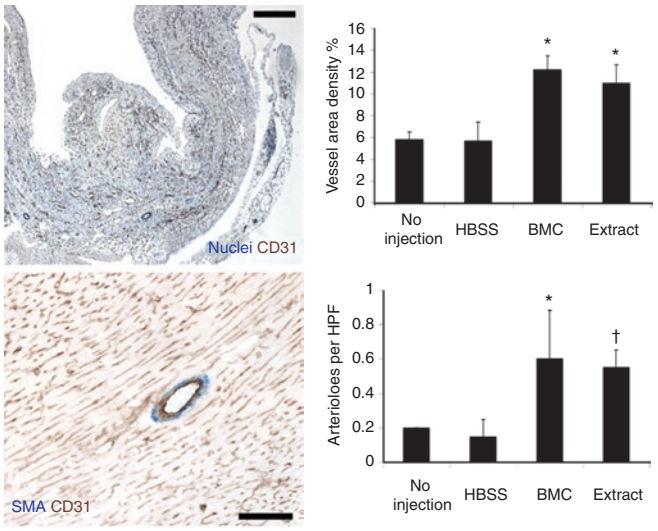

Figure 5 Enhanced vascularity at the infarct BZ. BMC and extract therapies result in both increased vessel density and number of smooth muscle-coated arterioles in the BZ. Bar (upper panel) = 300 µm, lower panel = 100 µm. *$P < 0.01$ versus HBSS and no injection. †$P < 0.01$ versus HBSS; $P < 0.001$ versus no injection. $N = 6$/group. BMC, bone marrow cells; BZ, border zone; HBSS, Hank's buffered saline solution; HPF, high-power field; SMA, α-smooth muscle actin.

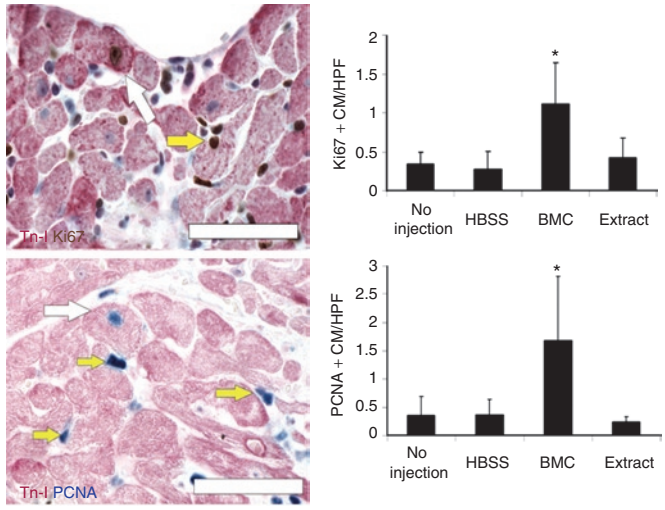

Figure 6 Cardiomyocyte proliferation. BMC therapy causes a significant increase in the number of cycling cardiomyocytes as demonstrated by increased numbers of Ki67$^+$ cardiomyocytes (upper panels) and PCNA$^+$ cardiomyocytes (lower panels). White arrows, apoptotic CMs; yellow arrows, apoptotic cells that are not CMs. Bar = 50 µm. $N = 6$/group. BMC, bone marrow cell; CM, cardiomyocyte; HPF, high-power field; PCNA, proliferating cell nuclear antigen; Tn-I, troponin-I.

Increased blood vessel density early after therapy

To gain insight as to how the functional benefits of BMCs and BMC extract were achieved, we quantified the capillary and arteriole density at day 6 post-MI. An additional control group included an MI group with no injections ($n = 6$) for comparison. Sections from the mid-papillary level were stained with antibodies against CD31 and α-smooth muscle actin. Both BMC and extract therapy resulted in significant increases in vascularity early after therapy (**Figure 5**) and there was no evidence of GFP expression within vessels. Extract injection increased total vessel area at infarct zone (12.7 ± 0.04% versus 4.4 ± 0.03%, $P = 0.006$) and BZ (12.2 ± 3.8% versus 4.3 ± 1.1%, $P = 0.001$) versus HBSS. Moreover, both BMC and extract therapies had a significantly higher number of arterioles in the BZ versus HBSS (0.60 ± 0.28 and 0.55 ± 0.10 versus 0.15 ± 0.10, $P < 0.007$, respectively). Vessel counts did not differ between any of the treated versus control groups in the remote zone. Interestingly, at day 28, neither vessel area, vessel length density (see **Supplementary Materials and Methods**), capillary number, nor arteriole number were significantly different among the HBSS, extract, and BMC groups. This suggests that the effects of intact BMCs and BMC extract on increasing vascularity are confined to the early time period after MI.

CM cycling and apoptosis early after therapy

At day 6 post-MI, BMC treatment increased the number of cycling CMs compared to the HBSS group, as determined by both proliferation marker (Ki67)/troponin-I double-staining (1.1 ± 0.5 versus 0.3 ± 0.2 Ki67$^+$ CM/high-power field (HPF), $P = 0.001$) and by proliferating cell nuclear antigen/troponin-I staining (1.7 ± 1.1 versus 0.4 ± 0.3 proliferating cell nuclear antigen positive CM/HPF, $P = 0.002$) (**Figure 6**). In contrast, extract therapy had no effect on CM cell cycling.

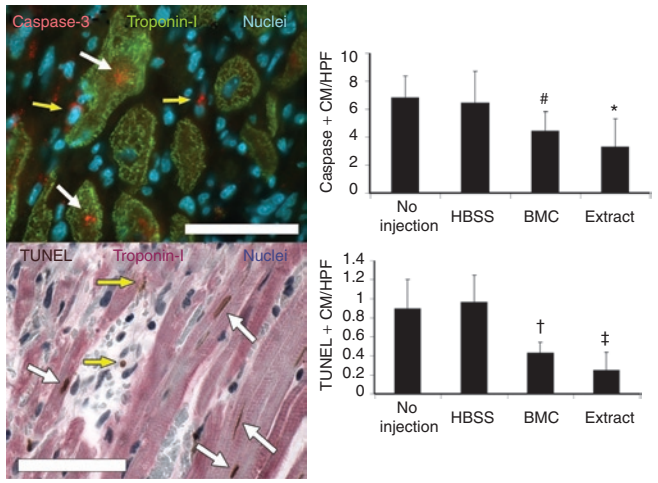

Figure 7 Reduction in CM apoptosis. Extract therapy causes a significant reduction in apoptotic CMs at the infarct BZ on day 6 post-MI. BMC therapy results in a strong trend toward fewer apoptotic CMs. White arrows, apoptotic CMs; yellow arrows, apoptotic cells that are not CMs. Bar = 50 µm. #$P = 0.05$ versus no injection and 0.08 versus HBSS; *$P < 0.01$ versus no injection and <0.05 versus HBSS; †$P = 0.04$ versus no injection and 0.07 versus HBSS; ‡$P = 0.011$ versus no injection and 0.02 versus HBSS. $N = 6$/group. BMC, bone marrow cells; BZ, border zone; CM, cardiomyocytes; MI, myocardial infarction; HBSS, Hank's buffered saline solution; HPF, high-power field; TUNEL, terminal deoxynucleotidyl transferase dUTP nick end labeling.

Extract therapy resulted in significant reduction in the number of apoptotic CMs at the BZ compared to HBSS injection, as determined by terminal deoxynucleotidyl transferase dUTP nick end labeling (TUNEL)/troponin-I (0.3 ± 0.3 versus 0.8 ± 0.5 TUNEL$^+$ CM/HPF, $P = 0.02$) and activated caspase-3/troponin-I staining (3.3 ± 2.0 versus 6.5 ± 2.2 caspase-3$^+$ CM/HPF, $P = 0.02$) (**Figure 7**). BMC therapy resulted in a trend of reduction in

© The American Society of Gene Therapy

apoptotic CMs (0.4 ± 0.3 TUNEL$^+$ CM/HPF $P = 0.07$; 4.4 ± 1.4 caspase-3$^+$ CM/HPF, $P = 0.08$) as well.

DISCUSSION

The major findings of this study are as follows.

1. Ultrasound-guided injections of whole BMCs or cell extract from the whole BM into mouse hearts 3 days post-MI in a total occlusion model result in improvement of cardiac function, a smaller infarct size, less LV remodeling, and an increase in the peri-infarct wall thickness.
2. The beneficial effects do not appear to be secondary to differentiation of the cells into CMs.
3. Persistence of cells does not appear to be necessary for improvement of cardiac function.
4. BMC extract, independent of the presence of live cells, has the ability to improve cardiac function, limit cardiac remodeling and result in less thinning of the peri-infarct myocardium.
5. Despite similar improvements in cardiac function at day 28 post-therapy, BMCs and BMC extract may exert their benefits via different mechanisms.

Experimental mouse models of MI are increasingly important for testing potential therapies for tissue repair such as gene transfer or stem cell delivery. The use of our ultrasound-guided closed-chest injection approach has overcome the high mortality associated with therapy several days after MI in the mouse model.[14] The ability to implant cells several days after induction of MI makes this model system relevant to current clinical trials, especially in light of recent reports indicating the benefits of delayed injections until ≥5 days after MI.[17] The reasons for this effect are unclear and may be due to changes in the tissue milieu after the infarct, but the result underscores the importance of being able to implant cells in mouse models at times similar to those used for clinical trial design. None of the mice in our experiment died during the closed-chest injections, reflecting both the efficacy and the safety of this image-guided approach.

Our results demonstrate that injection of unfractionated BMCs and cell extract attenuate adverse LV remodeling and improve cardiac function compared to controls. Both therapies resulted in smaller infarct scar and increased thickness of the peri-infarct myocardial wall. Under scrupulously controlled microscopy conditions that detect GFP while avoiding autofluorescence artifacts, we did not observe GFP-expressing CMs, capillaries, or arterioles in these BMC-implanted hearts, even under conditions that enable us to detect GFP$^+$ CMs in hearts from GFP transgenic mice. It must be emphasized that in our study protocol, we used whole BM and this contrasts with other studies that have used selected BM mononuclear cells and have reported either fusion or differentiation of BMCs into CMs.[18–21] Under our experimental conditions, we cannot exclude the possibility that improved cardiac function and limitation of infarct size may have resulted in part from mechanical support of the infarcted wall by the transplanted cells during critical earlier periods of remodeling, but differentiation into CMs at any reasonable level would have presumably been seen at the early time-point, or reflected in persistent GFP$^+$ CMs 1 month later. The improvement in LV systolic function resulting from injection of BMC extract, and the paucity of GFP-expressing cells at two separate time-points after therapy, strongly argue against differentiation and suggest a possible paracrine mechanism. In fact, implantation of cells into muscle typically results in a high level of cell death, and it is generally assumed that the surviving cells are responsible for the desired effect of the implantation. However, in this case, it is possible that the rare surviving GFP$^+$ cells detected in the infarct scar were irrelevant, and that it was the dead cells that were beneficial to cardiac function due to the bolus of growth factor delivery to surrounding tissue resulting from their demise.

To further explore the possibility of a paracrine influence on the blood vessels, we performed detailed analyses of vascularity both at an early time-point (day 3 post-therapy) and at the end of the study (day 28). Our results show that injection of BMCs or extract each increased vessel area density at the infarct BZ compared to control. Moreover, both BMC and extract therapies had a significantly higher number of arterioles in the BZ. In contrast, at day 28, no significant differences were detected between BMC, extract, and HBSS groups using four different vessel quantitation approaches, suggesting that the beneficial effects of both cell and extract therapy are seen early after the therapy is delivered while the overall cardiac functional benefits appear to last for a longer time period. These results are consistent with recent studies by Schuleri *et al.*,[22] who demonstrated that an early increase in myocardial perfusion resulted in longer term functional improvement. Increased vascularity during a critical early window in which BZ tissue is dying may save some of that tissue, resulting in a smaller scar size, even if the saved tissue ultimately acquires a normal vascularity profile and appears unremarkable at later times.

To further explore the possibility of paracrine effects on CM proliferation and apoptosis, we used Ki67 and proliferating cell nuclear antigen co-staining with troponin-I to identify CMs in cell cycle, and TUNEL and active caspase-3 co-staining with troponin-I to identify apoptotic CMs. Interestingly, our results suggest that at day 3 postinjection, BMC treatment increased the number of proliferating CMs compared to the HBSS group, but extract therapy had no effect on proliferation. Extract therapy resulted in significant reduction in the number of apoptotic CMs at the BZ versus HBSS while BMC therapy resulted in a trend of reduction in apoptotic CMs. Our findings thus suggest possible differences in the therapeutic mechanisms of intact cells versus cell extract. Extract therapy appears to act predominantly by reduction in apoptosis whereas BMC injection may induce CM proliferation with a trend toward less apoptotic cell death. It is enticing to speculate that the differences in proliferation and apoptosis seen between live BMC and extract therapies are due to a large single bolus of some paracrine factors delivered in the extract, compared to a slower release of that factor from the live BMCs. However, we cannot make such conclusions from these data, and further prospective timescale studies are needed to determine whether this is the case.

Although reports in the literature differ on whether BMCs differentiate into CMs when injected into infarcted mouse myocardium,[4,9,10] there is general agreement that such cell implantation results in some level of functional improvement.

© The American Society of Gene Therapy

The mechanism(s) underlying BMC therapy in animals and humans continues to be controversial. Our findings are consistent with several studies describing improvements in post-MI cardiac function in rodents following transplantation of several different cell types including BMCs, BM-derived mesenchymal stem cells, skeletal muscle myoblasts, and fetal CMs,[7,10,23–27] both in buffer and in gelling biopolymers.[28,29] These and other reports have suggested that implantation of various cell types may provide improvement through paracrine mechanisms leading to release of a wide array of cytokines that exert their effects on surrounding cells,[30–33] by improving perfusion to chronically ischemic tissue,[30] promoting survival of tenuous CMs,[7] or stimulating the proliferation of resident cardiac progenitor cells.[31] Our results confirm that live cells are not necessarily required to see the beneficial effects of BMC therapy and are consistent with the paracrine hypothesis of cellular repair strategies. Current clinical trials deliver selected BM mononuclear cells, but in our study, we report beneficial effects utilizing whole unselected BM and whole BM-derived extract. Isolation of the extract from more numerous types of cells in the whole BM will likely include more cytokines and paracrine factors. Additionally, compared to the use of cell-derived conditioned media which are obtained primarily from the active release of proteins and/or factors by living cells, the extract used in our study includes the proteins and/or factors that are also present within the cell and could be released passively to the surrounding tissue upon cell death. Our current on-going proteomics evaluation is aimed at identification of the proteins/factors within the extract to allow us to gain further insight into the possible mechanisms of cardiac functional improvement. Identification of the components of the extract will have important implications on the future development of novel molecular therapies with either a protein or a combination of proteins likely negating the need to inject live BMCs for therapeutic purposes post-MI.

MATERIALS AND METHODS

Animals and study groups. Male C57BL/6J (10–12 weeks old) mice were used for all experiments and handled according to the guidelines of the Institutional Animal Care and Use Committee.

MI and echocardiography. MI was surgically induced as previously described.[14] Briefly, infarction was induced by permanent ligation of the left anterior descending artery at ~50% of the length of the heart from the anterior–inferior edge of the left atrium to the apex.

Echocardiography was accomplished under isoflurane anesthesia with the use of a Vevo660 (VisualSonics, Toronto, Canada) equipped with a 30-MHz transducer.[14,34,35] Echocardiograms were obtained at baseline, 2 days post-MI (before injection), and at day 28 post-MI. We measured LVEF, end-systolic volume, end-diastolic volume, and wall thickness. Wall thickness was measured at the apical anterior wall (infarct wall thickness) and at the mid-anterior segment (peri-infarct wall thickness) separately on the parasternal long-axis view; posterior wall thickness was obtained at the papillary muscle level. Three cycles were measured for each assessment and the average values were obtained. The analyses of the echocardiography images were performed by two blinded reviewers.

Cell and extract preparation. BM was harvested from 15-week-old C57BL/6 mice that constitutively express GFP.[36] Briefly, the mouse BMCs were flushed from tibias and femurs with cold HBSS with 0.5% bovine serum albumin. The suspension was then strained through a 70-μm nylon filter and washed twice with HBSS/bovine serum albumin. The concentration of the cells was adjusted to 10^5 viable cells/μl. The viability of BMCs was checked using Trypan Blue with an average of 95% viability before injection. Cell-free extract was prepared by subjecting the BMCs to three freeze–thaw cycles using an ethanol/dry ice bath, followed by microcentrifugation at 14,000 rpm to remove insoluble material.

Ultrasound-guided injections. Animals received ultrasound-guided injection of BMCs (n = 14), BMC extract (n = 14), or HBSS/bovine serum albumin (n = 14) into myocardium as previously described.[14] Each heart was injected at day 3 post-MI with 10 μl of 1×10^6 cells, or the extract from 1×10^6 cells in 10 μl, or 10 μl HBSS/bovine serum albumin, divided into two 5-μl injections into the anterior wall. All animals were judged to be optimally injected and none of the animals needed to be removed from the study due to poor injection into the LV cavity.

Tissue analysis. Tissue was analyzed by two blinded reviewers and the average of the two analyses is reported at day 28 for the animals described. Infarct size was measured histologically as previously described.[34] To assess for histologic changes early after each therapy, additional animals (n = 6/group) were included and killed at day 6 post-MI (*i.e.*, day 3 post-therapy). Methods are described in detail in **Supplementary Materials and Methods**. Briefly, sections from the mid-ventricular level were examined for blood vessel density and arteriole count using antibodies to CD31 (Biocare, Concord, CA) and α-smooth muscle actin (Sigma-Aldrich, St Louis, MO). Blood vessel density was analyzed using ImagePro software (MediaCybernetics, Bethesda, MD) to detect the area of CD31 staining in the infarct zone, the BZ, and the remote myocardium. Arterioles defined as $CD31^+$ vessels with an α-smooth muscle actin coating were manually counted in each region. Capillaries were also quantified manually at day 28 using BS1 isolectin B4 staining (see **Supplementary Materials and Methods**).

Sections from the mid-ventricular level were examined for the presence of CMs that were undergoing apoptosis or were in cell cycle. Apoptosis was detected by two complementary methods: the colocalization of antibody staining for cardiac troponin-I (Abcam, Cambridge, MA) and TUNEL staining (ApopTag; Chemicon, Temecula, CA) within the same cell, and the colocalization of antibody staining for activated caspase-3 (BD Pharmingen, San Jose, CA) and for cardiac troponin-I within the same cell. CMs in cell cycle were detected using two complementary methods: co-staining for troponin-I and Ki67 (antibody from DAKO, Carpinteria, CA) within the same cell, and co-staining for troponin-I and proliferating cell nuclear antigen (antibody from Biocare) within the same cell. These apoptotic and cycling CMs were quantified by blinded reviewers counting the number of positive cells in five HPFs in the infarct zone, BZ, and the remote myocardium.

Histological detection of GFP. More details are in the **Supplementary Materials and Methods**. Briefly, hearts destined for histological staining for GFP were perfusion fixed before harvest. At day 28 post-MI, GFP^+ cells were detected by both direct intrinsic fluorescence and by immunostaining using a rabbit polyclonal antibody against GFP (Invitrogen, Carlsbad, CA/Molecular Probes, Eugene, OR), followed by a secondary goat anti-rabbit IgG conjugated to Alexa Fluor 660 (far-red emission). A tertiary donkey anti-goat IgG conjugated to Alexa Fluor 488 (green emission) was applied for further amplification of the green signal. Colorimetric detection of GFP was also performed, using a rabbit polyclonal antibody against GFP (Molecular Probes) and an horseradish peroxidase–conjugated goat anti-rabbit secondary IgG (ImmunoVision Technologies, Brisbane, CA). Color was developed with 3,3′-diaminobenzidine. Negative staining controls lacking primary antibody were performed, as were control staining of tissue from mice into which GFP^+ cells had not been injected. Tissues harvested at day 6 were analyzed for the presence of GFP^+ cells using antibodies against GFP (Invitrogen) developed with Ferangi Blue chromogen, and the

© The American Society of Gene Therapy

tissues were co-stained for troponin-I (Abcam). Tissues were examined for the presence of cells staining for both GFP and troponin-I, whose presence would suggest differentiation of injected BMCs into CMs.

RT-PCR. Whole hearts were harvested, frozen in liquid nitrogen, and subsequently homogenized with 7-mm zirconia beads in an SH-100 disruptor (Kurabo, Osaka, Japan) for 1 minute at 1,600 rpm into Trizol reagent (Invitrogen). RT was performed using a Superscript II First-Strand Synthesis Kit (Invitrogen). PCR of positive and negative controls was carried out from 1.0-μg template complementary DNA using an Advantage 2 PCR kit (Clontech, Palo Alto, CA) using the following conditions: 94 °C 30 seconds, 65 °C 30 seconds, 72 °C 30 seconds × 35 cycles. GFP primers were 5′-TGAACCGCATCGAGCTGAAG GG-3′ forward and 5′-TCCAGCAGGACCATGTGATCGC-3′ reverse. Hypoxanthine phosphoribosyltransferase reference gene primers were 5′-AAGGACCTCTCGAAGTGTTGGATA-3′ forward and 5′-CATTTAA AAGGAACTGTTGACAACG-3′ reverse. Qualitative RT-PCR using the TaqMan method was performed by the UCSF Helen Diller Family Comprehensive Cancer Center Genome Analysis Core facility using 25-ng template complementary DNA. GFP sequences were 5′-CGTAAA CGGCCACAAGTTCAG-3′ forward primer, 5′-GGGTGAGCTTGCCGT AGGT-3′ reverse primer, and 5′-CGCCCTCGCCCTCGC-3′ probe. Histone 3.3A reference sequences were 5′-GCTTCCAGAGCGCAGCTATC-3′ forward primer, 5′-GGCGTGCTAGCTGGATGTCT-3′ reverse primer, and 5′-TGCTTTGCAGGAGGCAAGTGAGGC-3′ probe.

Statistical analyses. Data were presented as mean ± SD. For the comparison between groups, an analysis of variance with Fisher's post hoc test was used. For the comparison within each group, paired *t*-test was used. A P value of <0.05 was considered significant.

SUPPLEMENTARY MATERIAL

Figure S1. Multi-color immunofluorescence approach screens out false positive green cardiomyocytes.

Figure S2. Dependence of GFP signal on fixation conditions.

Materials and Methods.

ACKNOWLEDGMENTS

This work was supported in part by the UCSF Cardiac Stem Cell Foundation to Y.Y.; a grant from the Wayne and Gladys Valley Foundation to W.G.; a grant from the UCSF Research Evaluation and Allocation Committee to M.L.S., and National Institute of Health grants R03EB005802 and R01HL086917 to M.L.S. and Y.Y. The authors declare no competing financial interests.

REFERENCES

1. Losordo, DW and Dimmeler, S (2004). Therapeutic angiogenesis and vasculogenesis for ischemic disease: part II: cell-based therapies. *Circulation* **109**: 2692–2697.
2. Wollert, KC and Drexler, H (2005). Clinical applications of stem cells for the heart. *Circ Res* **96**: 151–163.
3. Rosenzweig, A (2006). Cardiac cell therapy—mixed results from mixed cells. *N Engl J Med* **355**: 1274–1277.
4. Balsam, LB, Wagers, AJ, Christensen, JL, Kofidis, T, Weissman, IL and Robbins, RC (2004). Haematopoietic stem cells adopt mature haematopoietic fates in ischaemic myocardium. *Nature* **428**: 668–673.
5. Jackson, KA, Majka, SM, Wang, H, Pocius, J, Hartley, CJ, Majesky, MW *et al.* (2001). Regeneration of ischemic cardiac muscle and vascular endothelium by adult stem cells. *J Clin Invest* **107**: 1395–1402.
6. Janssens, S, Dubois, C, Bogaert, J, Theunissen, K, Deroose, C, Desmet, W *et al.* (2006). Autologous bone marrow-derived stem-cell transfer in patients with ST-segment elevation myocardial infarction: double-blind, randomised controlled trial. *Lancet* **367**: 113–121.
7. Kocher, AA, Schuster, MD, Szabolcs, MJ, Takuma, S, Burkhoff, D, Wang, J *et al.* (2001). Neovascularization of ischemic myocardium by human bone-marrow-derived angioblasts prevents cardiomyocyte apoptosis, reduces remodeling and improves cardiac function. *Nat Med* **7**: 430–436.
8. Lunde, K, Solheim, S, Aakhus, S, Arnesen, H, Abdelnoor, M, Egeland, T *et al.* (2006). Intracoronary injection of mononuclear bone marrow cells in acute myocardial infarction. *N Engl J Med* **355**: 1199–1209.
9. Murry, CE, Soonpaa, MH, Reinecke, H, Nakajima, H, Nakajima, HO, Rubart, M *et al.* (2004). Haematopoietic stem cells do not transdifferentiate into cardiac myocytes in myocardial infarcts. *Nature* **428**: 664–668.
10. Orlic, D, Kajstura, J, Chimenti, S, Jakoniuk, I, Anderson, SM, Li, B *et al.* (2001). Bone marrow cells regenerate infarcted myocardium. *Nature* **410**: 701–705.
11. Schächinger, V, Erbs, S, Elsässer, A, Haberbosch, W, Hambrecht, R, Hölschermann, H *et al.* (2006). Improved clinical outcome after intracoronary administration of bone-marrow-derived progenitor cells in acute myocardial infarction: final 1-year results of the REPAIR-AMI trial. *Eur Heart J* **27**: 2775–2783.
12. Dawn, B and Bolli, R (2005). Adult bone marrow-derived cells: regenerative potential, plasticity, and tissue commitment. *Basic Res Cardiol* **100**: 494–503.
13. Kajstura, J, Rota, M, Whang, B, Cascapera, S, Hosoda, T, Bearzi, C *et al.* (2005). Bone marrow cells differentiate in cardiac cell lineages after infarction independently of cell fusion. *Circ Res* **96**: 127–137.
14. Springer, ML, Sievers, RE, Viswanathan, MN, Yee, MS, Foster, E, Grossman, W *et al.* (2005). Closed-chest cell injections into mouse myocardium guided by high-resolution echocardiography. *Am J Physiol Heart Circ Physiol* **289**: H1307–H1314.
15. Yang, F, Liu, YH, Yang, XP, Xu, J, Kapke, A and Carretero, OA (2002). Myocardial infarction and cardiac remodelling in mice. *Exp Physiol* **87**: 547–555.
16. Brazelton, TR and Blau, HM (2005). Optimizing techniques for tracking transplanted stem cells in vivo. *Stem Cells* **23**: 1251–1265.
17. Schächinger, V, Erbs, S, Elsässer, A, Haberbosch, W, Hambrecht, R, Hölschermann, H *et al.* (2006). Intracoronary bone marrow-derived progenitor cells in acute myocardial infarction. *N Engl J Med* **355**: 1210–1221.
18. Kamihata, H, Matsubara, H, Nishiue, T, Fujiyama, S, Tsutsumi, Y, Ozono, R *et al.* (2001). Implantation of bone marrow mononuclear cells into ischemic myocardium enhances collateral perfusion and regional function via side supply of angioblasts, angiogenic ligands, and cytokines. *Circulation* **104**: 1046–1052.
19. Scorsin, M, Hagege, AA, Dolizy, I, Marotte, F, Mirochnik, N, Copin, H *et al.* (1998). Can cellular transplantation improve function in doxorubicin-induced heart failure?. *Circulation* **98**(19 Suppl): II151–II155; discussion II155.
20. Strauer, BE, Brehm, M, Zeus, T, Köstering, M, Hernandez, A, Sorg, RV *et al.* (2002). Repair of infarcted myocardium by autologous intracoronary mononuclear bone marrow cell transplantation in humans. *Circulation* **106**: 1913–1918.
21. Zhang, S, Guo, J, Zhang, P, Liu, Y, Jia, Z, Ma, K *et al.* (2004). Long-term effects of bone marrow mononuclear cell transplantation on left ventricular function and remodeling in rats. *Life Sci* **74**: 2853–2864.
22. Schuleri, KH, Amado, LC, Boyle, AJ, Centola, M, Saliaris, AP, Gutman, MR *et al.* (2008). Early improvement in cardiac tissue perfusion due to mesenchymal stem cells. *Am J Physiol Heart Circ Physiol* **294**: H2002–H2011.
23. Etzion, S, Battler, A, Barbash, IM, Cagnano, E, Zarin, P, Granot, Y *et al.* (2001). Influence of embryonic cardiomyocyte transplantation on the progression of heart failure in a rat model of extensive myocardial infarction. *J Mol Cell Cardiol* **33**: 1321–1330.
24. Scorsin, M, Hagège, A, Vilquin, JT, Fiszman, M, Marotte, F, Samuel, JL *et al.* (2000). Comparison of the effects of fetal cardiomyocyte and skeletal myoblast transplantation on postinfarction left ventricular function. *J Thorac Cardiovasc Surg* **119**: 1169–1175.
25. Toma, C, Pittenger, MF, Cahill, KS, Byrne, BJ and Kessler, PD (2002). Human mesenchymal stem cells differentiate to a cardiomyocyte phenotype in the adult murine heart. *Circulation* **105**: 93–98.
26. Amado, LC, Saliaris, AP, Schuleri, KH, St John, M, Xie, JS, Cattaneo, S *et al.* (2005). Cardiac repair with intramyocardial injection of allogeneic mesenchymal stem cells after myocardial infarction. *Proc Natl Acad Sci USA* **102**: 11474–11479.
27. Thompson, RB, van den Bos, EJ, Davis, BH, Morimoto, Y, Craig, D, Sutton, BS *et al.* (2005). Intracardiac transplantation of a mixed population of bone marrow cells improves both regional systolic contractility and diastolic relaxation. *J Heart Lung Transplant* **24**: 205–214.
28. Christman, KL, Fok, HH, Sievers, RE, Fang, Q and Lee, RJ (2004). Fibrin glue alone and skeletal myoblasts in a fibrin scaffold preserve cardiac function after myocardial infarction. *Tissue Eng* **10**: 403–409.
29. Christman, KL and Lee, RJ (2006). Biomaterials for the treatment of myocardial infarction. *J Am Coll Cardiol* **48**: 907–913.
30. Gnecchi, M, He, H, Liang, OD, Melo, LG, Morello, F, Mu, H *et al.* (2005). Paracrine action accounts for marked protection of ischemic heart by Akt-modified mesenchymal stem cells. *Nat Med* **11**: 367–368.
31. Kinnaird, T, Stabile, E, Burnett, MS, Shou, M, Lee, CW, Barr, S *et al.* (2004). Local delivery of marrow-derived stromal cells augments collateral perfusion through paracrine mechanisms. *Circulation* **109**: 1543–1549.
32. Mangi, AA, Noiseux, N, Kong, D, He, H, Rezvani, M, Ingwall, JS *et al.* (2003). Mesenchymal stem cells modified with Akt prevent remodeling and restore performance of infarcted hearts. *Nat Med* **9**: 1195–1201.
33. Uemura, R, Xu, M, Ahmad, N and Ashraf, M (2006). Bone marrow stem cells prevent left ventricular remodeling of ischemic heart through paracrine signaling. *Circ Res* **98**: 1414–1421.
34. Takagawa, J, Zhang, Y, Wong, ML, Sievers, RE, Kapasi, NK, Wang, Y *et al.* (2007). Myocardial infarct size measurement in the mouse chronic infarction model: comparison of area- and length-based approaches. *J Appl Physiol* **102**: 2104–2111.
35. Zhang, Y, Takagawa, J, Sievers, RE, Khan, MF, Viswanathan, MN, Springer, ML *et al.* (2007). Validation of the wall motion score and myocardial performance indexes as novel techniques to assess cardiac function in mice after myocardial infarction. *Am J Physiol Heart Circ Physiol* **292**: H1187–H1192.
36. Okabe, M, Ikawa, M, Kominami, K, Nakanishi, T and Nishimune, Y (1997). 'Green mice' as a source of ubiquitous green cells. *FEBS Lett* **407**: 313–319.